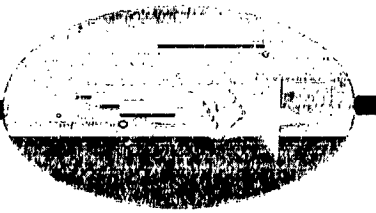

Lockheed

Missiles & Space Company, Inc.

HUNTSVILLE RESEARCH & ENGINEERING CENTER

Cummings Research Park
4800 Bradford Drive,
Huntsville, Alabama

SPACE SHUTTLE CONTAMINATION DUE TO BACKFLOW FROM CONTROL MOTOR EXHAUST

FINAL REPORT

October 1976

Contract NAS8-31440

Prepared for National Aeronautics and Space Administration
Marshall Space Flight Center, Alabama 35812

by

S. J. Robertson
S. T. K. Chan
A. L. Lee

APPROVED: B. Hobson Shirley

B. Hobson Shirley, Supervisor
Engineering Sciences Section

for J. S. Farrior
Resident Director

FOREWORD

This document is the final report for Contract NAS8-31440, "Space Shuttle Contamination Due to Backflow from Control Motor Exhaust." The contract was initiated on 10 April 1975 as a 10-month effort to develop analytical techniques for predicting the back-scattering of out gas contamination due to outgassing from an orbiting spacecraft. The contract was later extended an additional eight months to perform analytical studies of molecular scattering due to the vernier and flash evaporator plumes impinging on the Space Shuttle Orbiter wings.

The results of the first 10-month effort were documented in an Interim Report.* The results of the remaining 8-month effort are documented in this final report.

The study was performed by personnel of the Lockheed Missiles & Space Company, Inc., Huntsville Research & Engineering Center, for the Space Sciences Laboratory of NASA-Marshall Space Flight Center. The NASA Technical Monitor is Dr. R. J. Naumann. The interest of Dr. Naumann in these studies has been greatly appreciated.

*Robertson, S. J., "Space Self-Contamination Due to Back-Scattering of Outgas Products," LMSC-HREC TR D496676, Lockheed Missiles & Space Company, Inc., Huntsville, Ala., January 1976.

CONTENTS

1. INTRODUCTION AND SUMMARY

The studies reported in this document are concerned with aspects of the overall problem generally referred to as spacecraft contamination. The Space Shuttle orbiter and accompanying Spacelab payloads are the particular spacecraft with which these studies are concerned. The following two specific problems were addressed. The first concerned the scattering of molecules from the vernier engines and flash evaporator nozzle after impingement on the orbiter wing surfaces. The scattered molecules may pass before the field of view of optical instruments, thus possibly obscuring observations. This problem was considered in a previous study reported in Ref. 1. This previous study, however, was somewhat simplified in that collisions between the scattered molecules and the plume flow field were not considered. The purpose of the present study was to specifically consider the effect of these collisions. The results of the study show that the effect of the collisions is to reduce the predicted column densities due to vernier engine firings by up to 90% depending on the location and orientation of the vernier engine and direction of the line of sight (LOS).

The second problem dealt with in these studies concerned the backflow of molecules out of the flash evaporator nozzle plume flow field due to intermolecular collisions in the plume. A method was formulated for dealing with this problem and results were obtained which compared surprisingly well with experiment data. More reliable testing is needed to judge the accuracy of the theoretical results.

Detailed results of these studies are given in the following sections.

2. MOLECULAR SCATTERING FROM ORBITER WING

The analytical method employed in this study is based on the BGK model first described by Bhatnagar et al (Ref. 1). The application in the present analysis is similar to a previous application described in Ref. 2. The BGK model kinetic equation for this application is

$$\vec{v} \cdot \frac{\partial f_1}{\partial \vec{r}} = \nu (M - f_1) \tag{2.1}$$

where f_1 is the distribution function for the molecules flowing from the jet under consideration. We assume that the molecules flow from the jet location to the orbiter wing surface where it reflects according to a Lambertian (cosine law) directional distribution. Some of the reflected molecules then travel from the surface to the LOS for which column densities are being computed. Enroute from the wing surface to the LOS, collisions occur with the jet plume flow field and the ambient atmosphere. The collision processes are such that the molecules are either overwhelmingly scattered in the direction of the jet flow or the ambient flow, depending on whether the collisions are with the jet flow field or the ambient atmosphere. The collided molecules are thus primarily deflected away from the LOS and may be regarded as lost. The quantity M in Eq. (2.1), which accounts for the further travels of these deflected molecules, may therefore be set to zero. The quantity ν is the total collision frequency which includes both collisions with the jet plume and the ambient atmosphere. The total collision frequency ν may be expressed as the sum of the two separate collision rates:

$$\nu = \nu_{11} + \nu_{12} \tag{2.2}$$

where ν_{11} is the collision rate with the jet plume, and ν_{12} is the collision rate with the ambient atmosphere. These collision rates are given by (Ref. 2).

$$\nu_{11} = 1.023 \frac{\dot{m}_1}{m_1} \sigma_{11} \tag{2.3}$$

and

$$\nu_{12} = 1.023\, n_2\, u_2\, \sigma_{12} \tag{2.4}$$

where $\dot{m}_1$ is the jet plume mass flow rate per unit area at a point in the flow field, m_1 is the molecular mass of the molecules in the jet plume, σ_{11} is the cross section for collisions between jet molecules reflected from the wing and molecules in the plume flow field, n_2 is the number density of molecules in the ambient atmosphere, u_2 is the ambient flow velocity and σ_{12} is the cross section for collisions between jet molecules reflected from the wing and molecules in the ambient atmosphere.

Integrating Eq. (2.1) for the distribution function at a point in the LOS yields

$$\bullet f_1 (\vec{v}, \vec{r}) = f_1 (\vec{v}, \vec{r}_w) \exp\left[- \frac{1}{|\vec{v}|} \int_{\vec{r}_w}^{\vec{r}} \nu(\vec{r}') \left| d\vec{r}' \right| \right] \tag{2.5}$$

where $\vec{r}_w$ is a point on the wing surface and $f_1 (\vec{v}, \vec{r}_w)$ is the distribution function of the reflected molecules at the wing surface. The function of $f_1 (\vec{v}, \vec{r}_w)$ is known from the flux rate incident on the surface and the cosine law reflectior pattern:

$$f_1(\vec{v}, \vec{r}_w) = \frac{2}{\pi} \frac{\dot{m}_1(\vec{r}_w) \left| \vec{n}_w \cdot \vec{e}_{j-w} \right|}{m_1} \left(\frac{m_1}{2kT_w} \right)^2 \exp\left(- \frac{m_1}{2kT_w} v^2 \right) \quad (2.6)$$

where $\vec{n}_w$ is a unit vector normal to the wing surface, $\vec{e}_{j-w}$ is a unit vector in the direction from the jet to the point $\vec{r}_w$ on the wing surface, k is Boltzmann's constant and T_w is the temperature of the wing surface. The local number density, n, is found by integrating Eq. (2.5) over all velocities and directions from the wing surface to the point on the LOS. After the velocities are integrated out, the remaining expression is:

$$n(\vec{r}) = \frac{1}{\sqrt{8\pi m k T_w}} \int_A \frac{\dot{m}(\vec{r}_w) \left| \vec{r}_w \cdot \vec{e}_{j-w} \right| \left| \vec{r}_w \cdot \vec{e}_{r-w} \right|}{r^2}$$

$$\cdot \exp\left[- \sqrt{\frac{m_1}{2kT_w}} \int \nu(r')\, dr' \right] dA \quad (2.7)$$

where $\vec{e}_{r-w}$ is a unit vector in the direction from the point $\vec{r}$ on the LOS to the point $\vec{r}_w$ on the wing surface, $\vec{r}$ is the distance from $\vec{r}$ to $\vec{r}_w$ and A is wing surface area. Equation (2.7) is integrated numerically.

The column density N is obtained by numerically integrating the number density n along the LOS from the prime measuring point (PMP) out to a point where the density has diminished to small values.

The orbiter geometry is represented in this analysis as a triangular shaped wing defined by the location of the three vertex points. In all the results presented in this document, the three vertices are: (760, 110, 376), (1500, 110, 296) and (1500, 480, 296) where (x,y,z) are the coordinates of the three points in inches according to the Shuttle orbiter vehicle coordinate system. In the numerical analysis, the wing is divided into elementary

triangles of the same shape and the integration carried out over the individual elements by assuming a linear variation of the integrand. The location of the PMP was taken to be (1107, 0, 507). The locations of both the Nos. 4 and 6 vernier engines were taken to be (1565, 134, 459), with the No. 4 directed in the -Z direction and the No. 6 directed in the +Y direction. The temperature of the wing surface T_w was assumed to be 300K. The flash evaporator nozzle was taken to be located at (1504, 126, 291), which is slightly below and to the rear of the wing trailing edge, and directed in the +Y direction.

Number densities and column densities were computed along LOS s from the PMP in the +Z direction and in a direction 60 deg from the +Z axis and 30 deg from the +Y axis in the YZ plane. In the vehicle coordinate system, the +X axis points in the aft direction, the +Y axis points in the starboard direction and the +Z axis points directly overhead. Results were obtained for the Nos. 4 and 6 vernier engines and the latest considered location of the flash evaporator.

Shown in Figs. 2-1 through 2-8 are computed number densities along a LOS in the +Z direction during firing of the No. 6 vernier engine at an orbit altitude of 400 km. The results shown in Fig. 2-1 are the total density, n, the contribution due to direct flow from the jet, n_d, and the contribution due to scattering from the wing, n_s. These results include attenuation effects due to collisions with both the jet plume flow field and the ambient atmosphere. The direct flow portion n_d is seen to be the primary contribution over the bulk of the LOS. Recall that this portion is attenuated only by collisions with the ambient atmosphere. The scattered portion n_s, on the other hand, is attenuated by collisions with both the jet plume and the ambient atmosphere, thus resulting in a relatively rapid decrease in density along the LOS. The same results are shown again in Fig. 2-1a with the additional shadowing of the cargo bay doors and fuselage. The contribution due to direct flow from the jet, n_d, is not reduced while the contribution due to the scattering off the wing, n_s, is greatly reduced, especially for the portion of the LOS near the

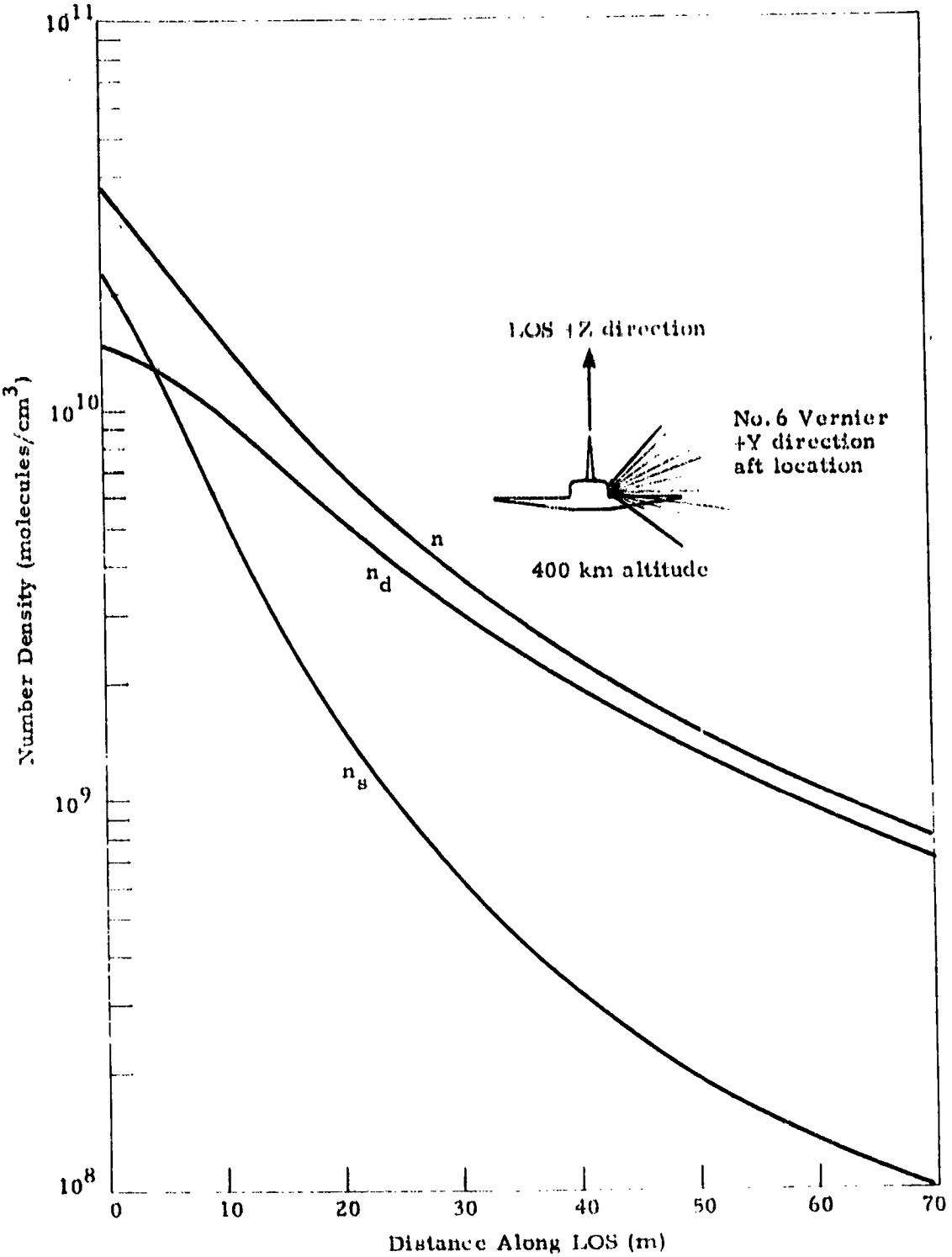

Fig. 2-1 - Computed Number Densities Along a Line-of-Slight Considering Collisions with the Jet Plume Flow Field and the Ambient Atmosphere

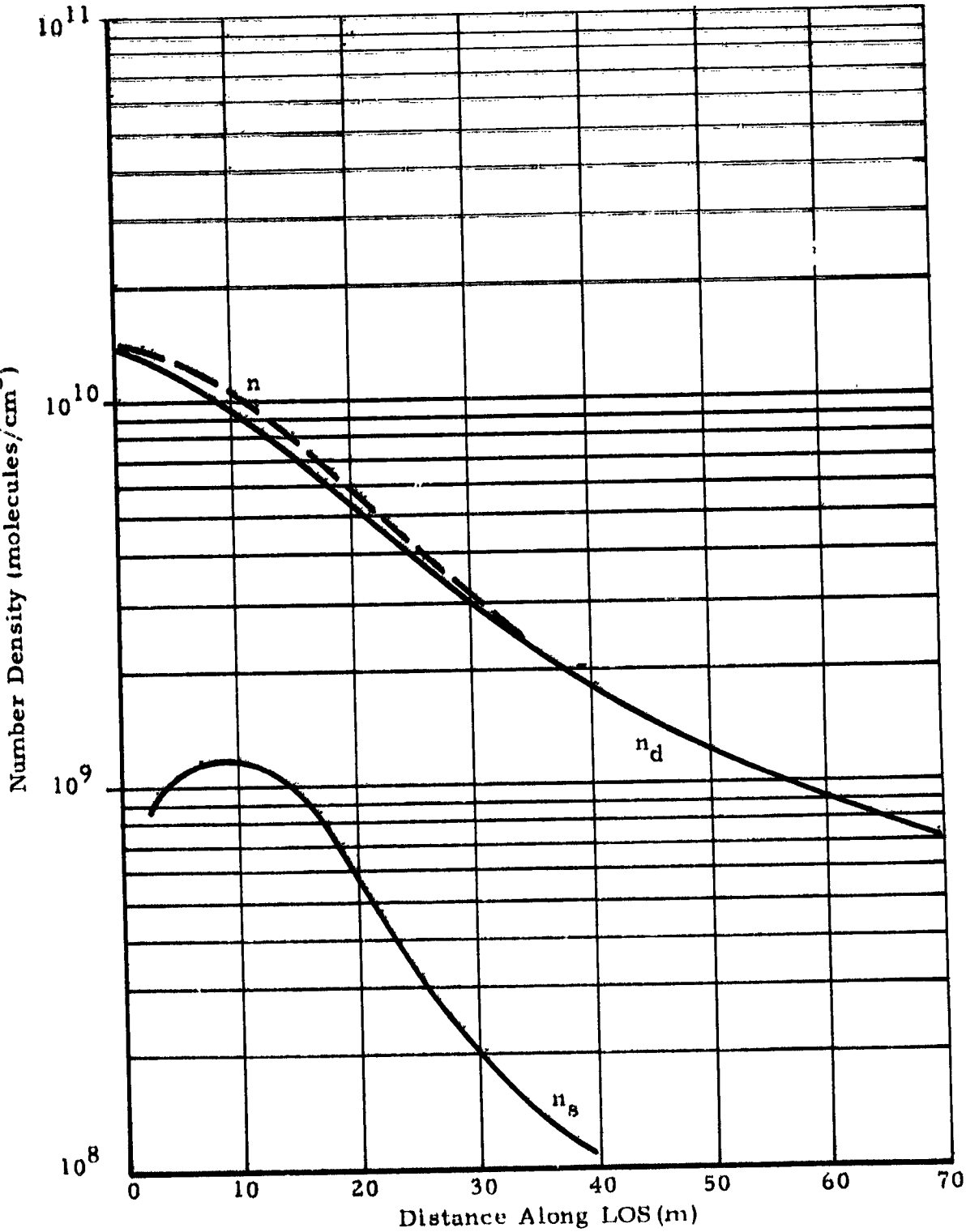

Fig. 2-1a - Computed Number Densities Along a Line of Sight Considering Collisions with the Jet Plume Field and Ambient Atmosphere and Shading Effects of Orbiter Geometry

PMP. The result is a reduced number density. At the location near the PMP the shadowing of the cargo bay doors and fuselage reduces the number density to less than one-third of the original value.

The same results are shown in Fig. 2-2 but without including any attenuation effects (the "o" subscript denotes zero molecular collisions). The direct flow contribution, n_{d_o}, is seen to not be changed appreciably, but the scattered contribution is increased substantially. Figure 2-2a shows the same results but including the shadowing effects of shuttle geometry. The scattered contribution is seen to be reduced drastically within 10 m of the PMP.

The same results are again shown in Fig. 2-3 but this time considering collisions only with the jet plume flow field (the "na" subscript denotes no atmospheric collisions). Comparing these results with Fig. 2-1 shows that atmospheric collisions at an orbit altitude of 400 km are not significant compared to collisions with the jet plume flow field. Figure 2-3a shows the additional effects of shading. The scattered amount is reduced by more than an order of magnitude.

The relative effects of considering collisions are also illustrated in Fig. 2-4 in which the portion scattered from the wing is shown without collisions (n_{s_o}), with collisions with the jet plume flow field only ($n_{s_{na}}$) and with collisions with both the jet plume flow field and ambient atmosphere (n_s). Again, collisions with the ambient atmosphere are shown to not be significant at 400 km altitude, but collisions with the jet plume flow field are shown to greatly reduce the computed densities. Figure 2-4a shows the effects of shading. The reduction of number densities is most drastic in the region within 20 meters of the PMP.

The effect of altitude on densities along the LOS is shown in Fig. 2-5. The densities in this figure are the total number densities including direct flow and scattered from the wing with collisions with both the jet plume flow

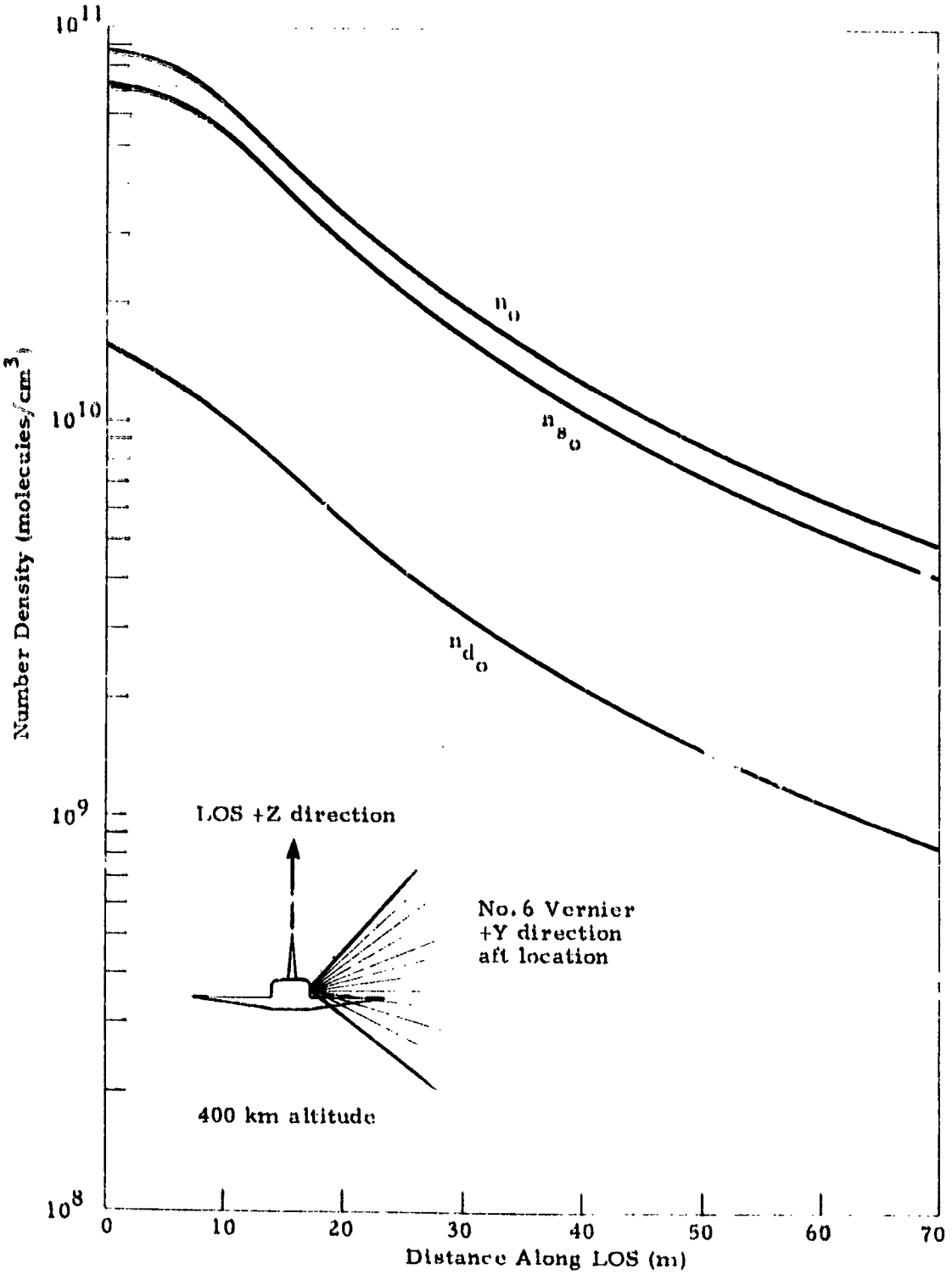

Fig. 2-2 - Computed Number Densities Along a Line-of-Sight Considering No Collisions with Either the Jet Plume Flow Field or the Ambient Atmosphere

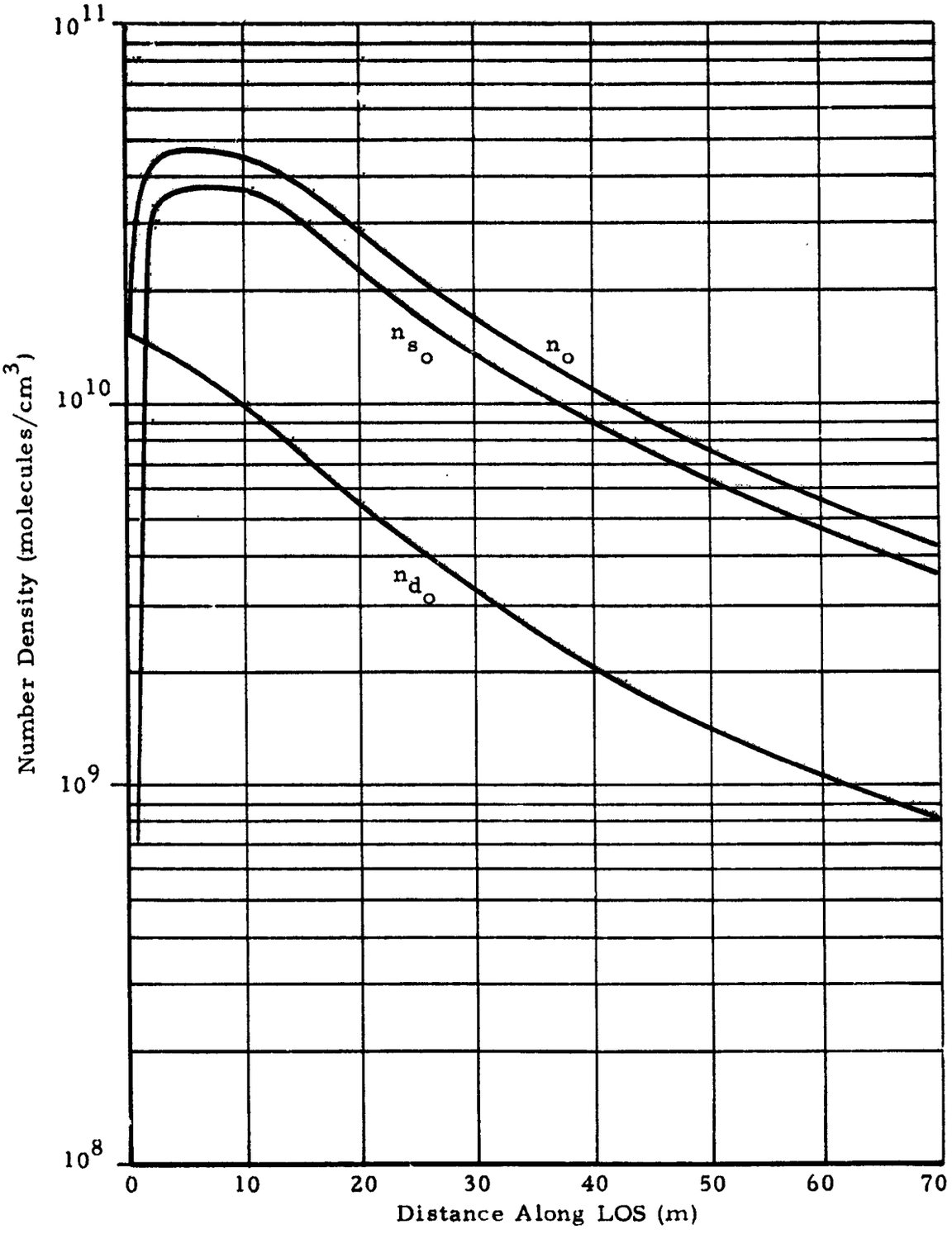

Fig. 2-2a - Computed Number Densities Along a Line of Sight Considering Collisions with Neither the Jet Plume Field Nor the Ambient Atmosphere but Including the Shading Effects of Orbiter Geometry

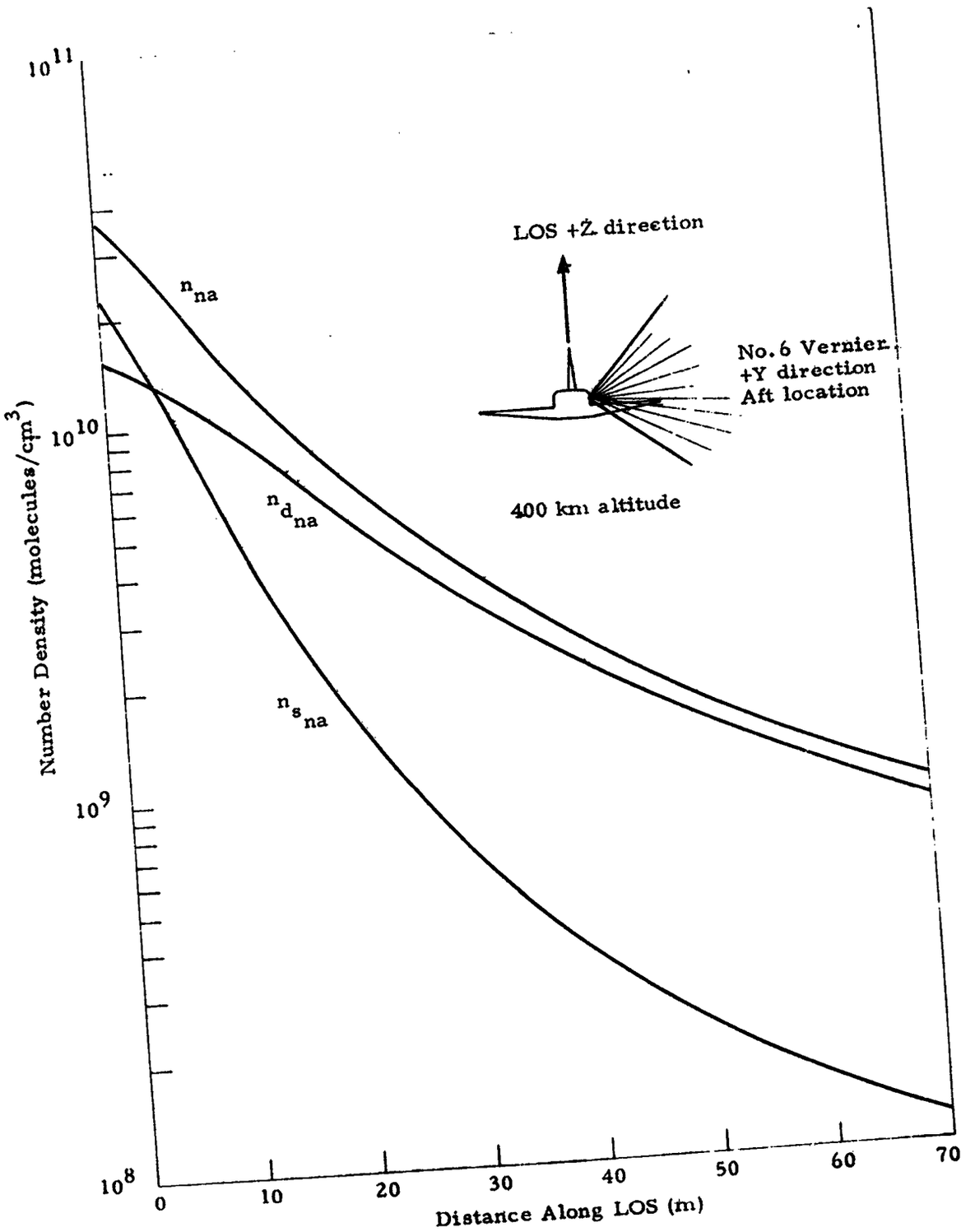

Fig. 2-3 - Computed Number Densities Along a Line-of-Sight Considering Collisions with the Jet Plume Flow Field Only

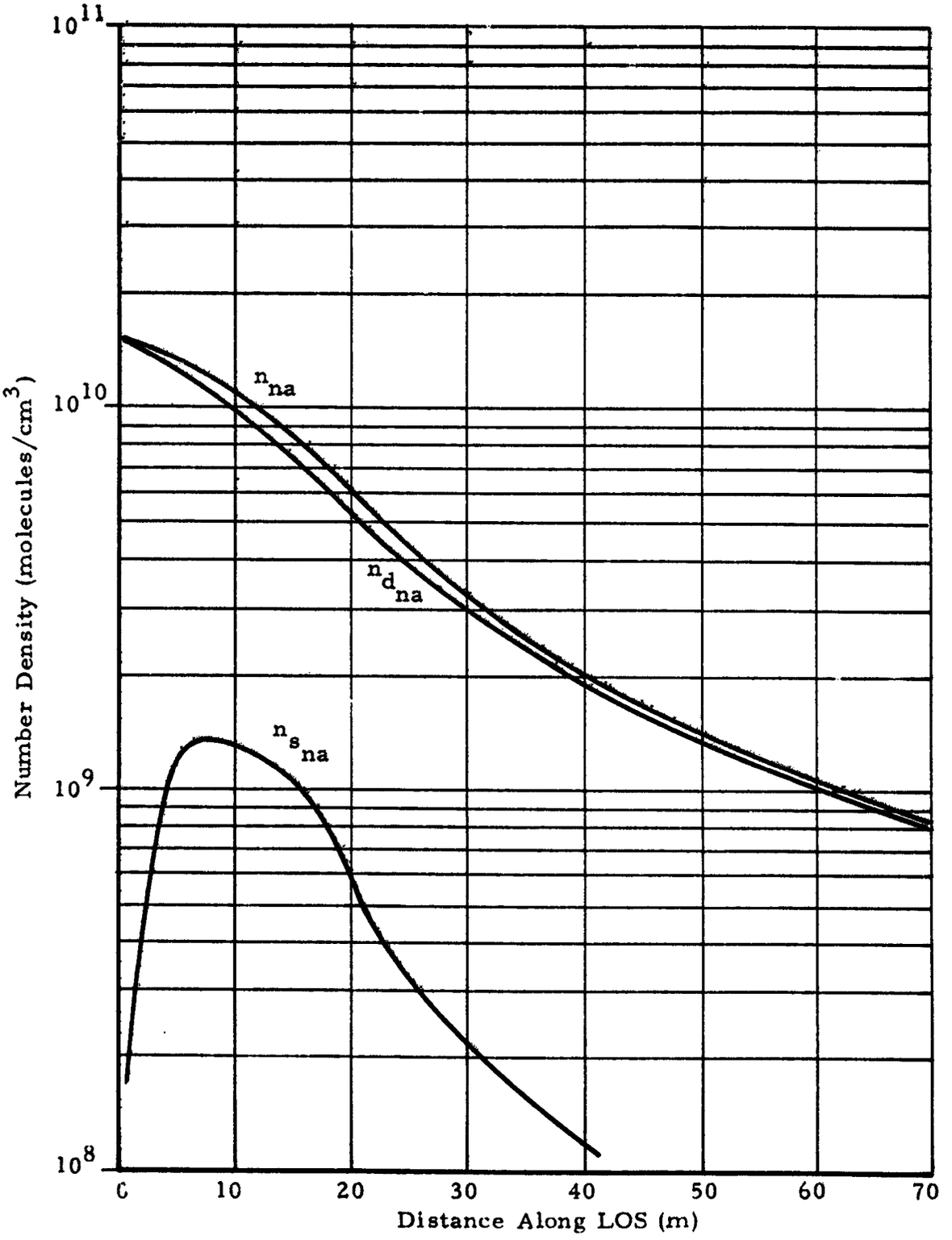

Fig. 2-3a - Computer Number Densities Along a Line of Sight Considering Collisions with the Jet Plume Flow Field Only and Shading Effects of Orbiter Geometry

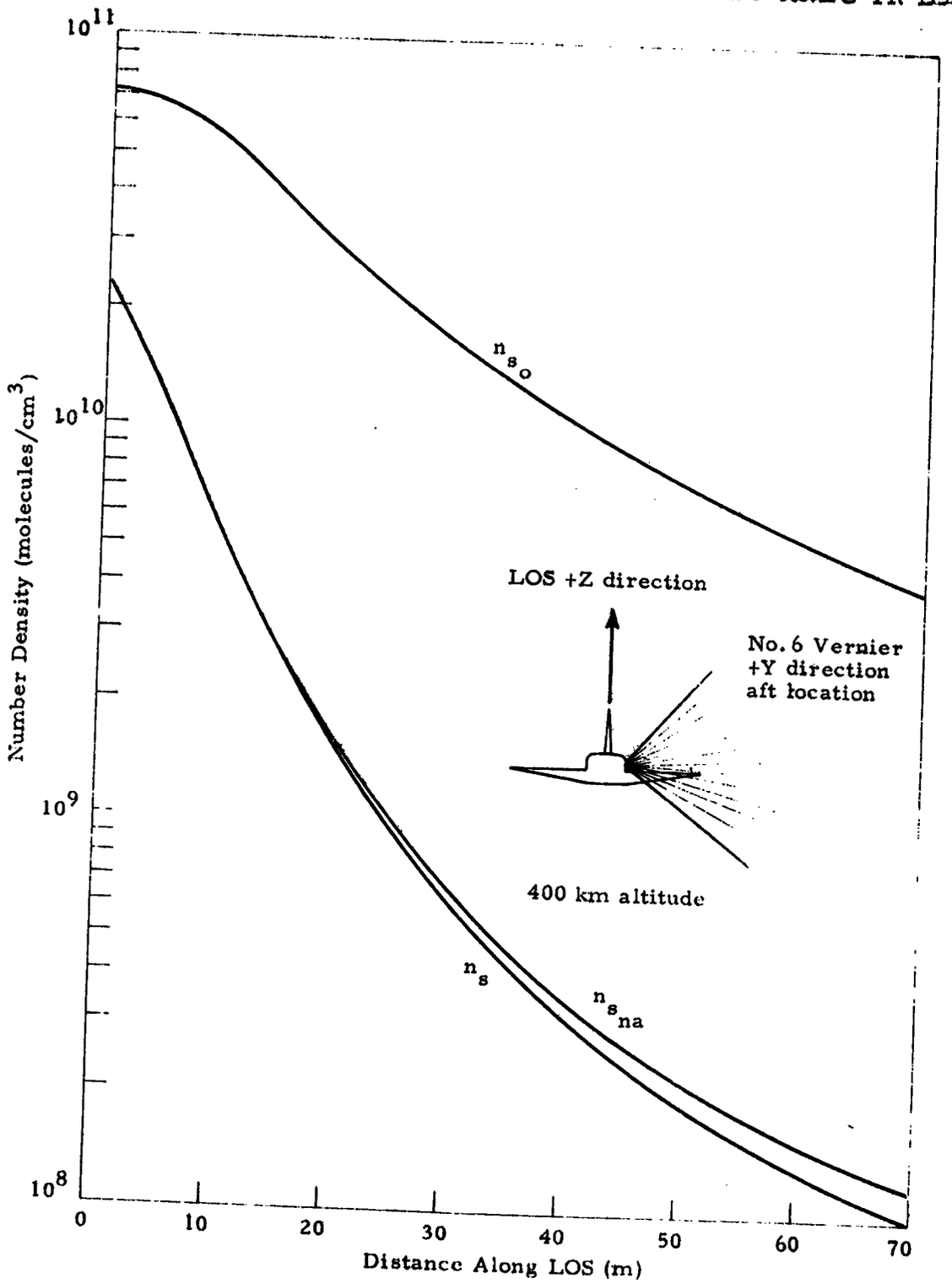

Fig. 2-4 - Computed Number Densities Along a Line-of-Sight for Molecules Scattered Off the Wing

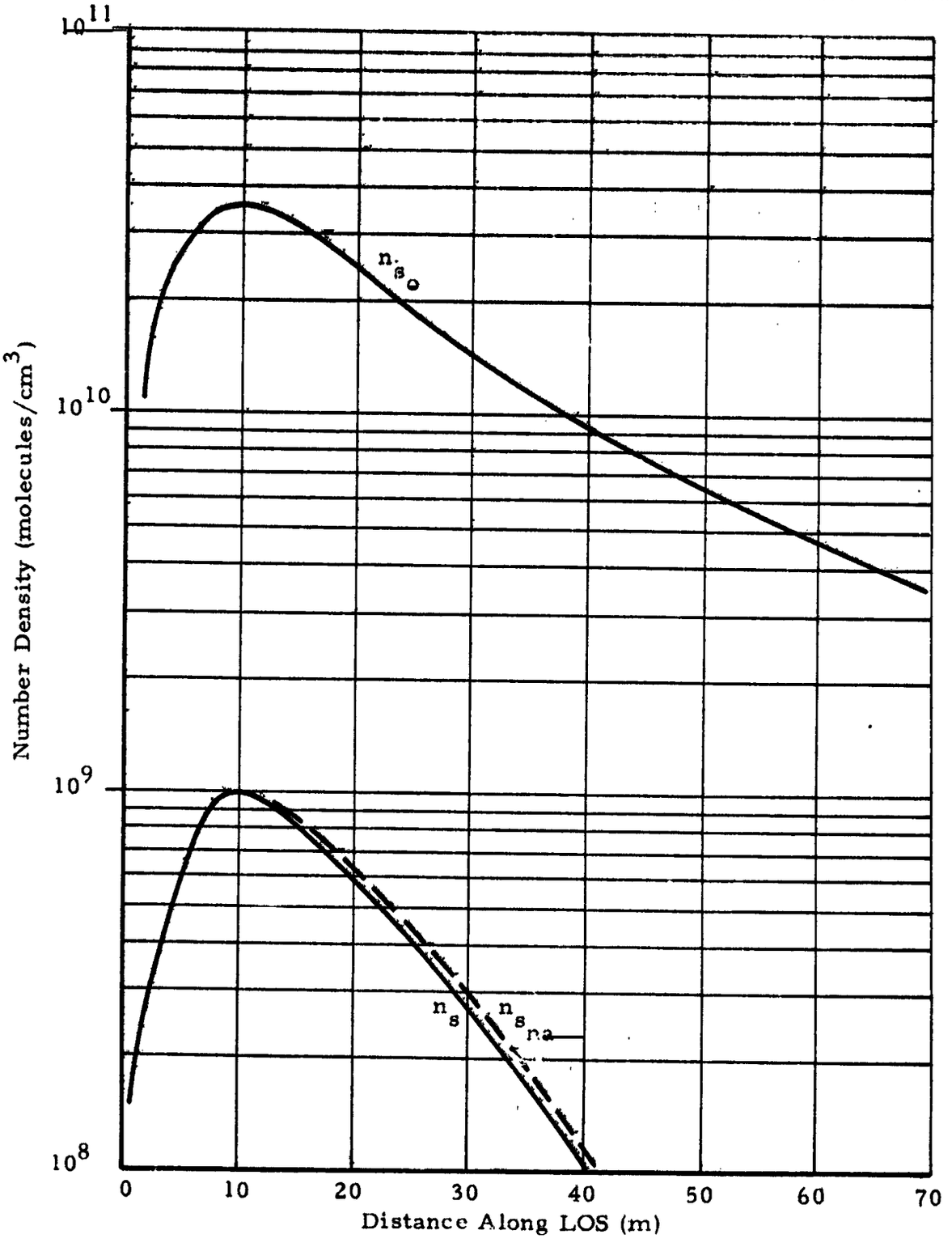

Fig. 2-4a - Computed Number Densities Along a Line of Sight for Molecules Scattered Off the Wing with Consideration of Orbiter Geometry Shadings

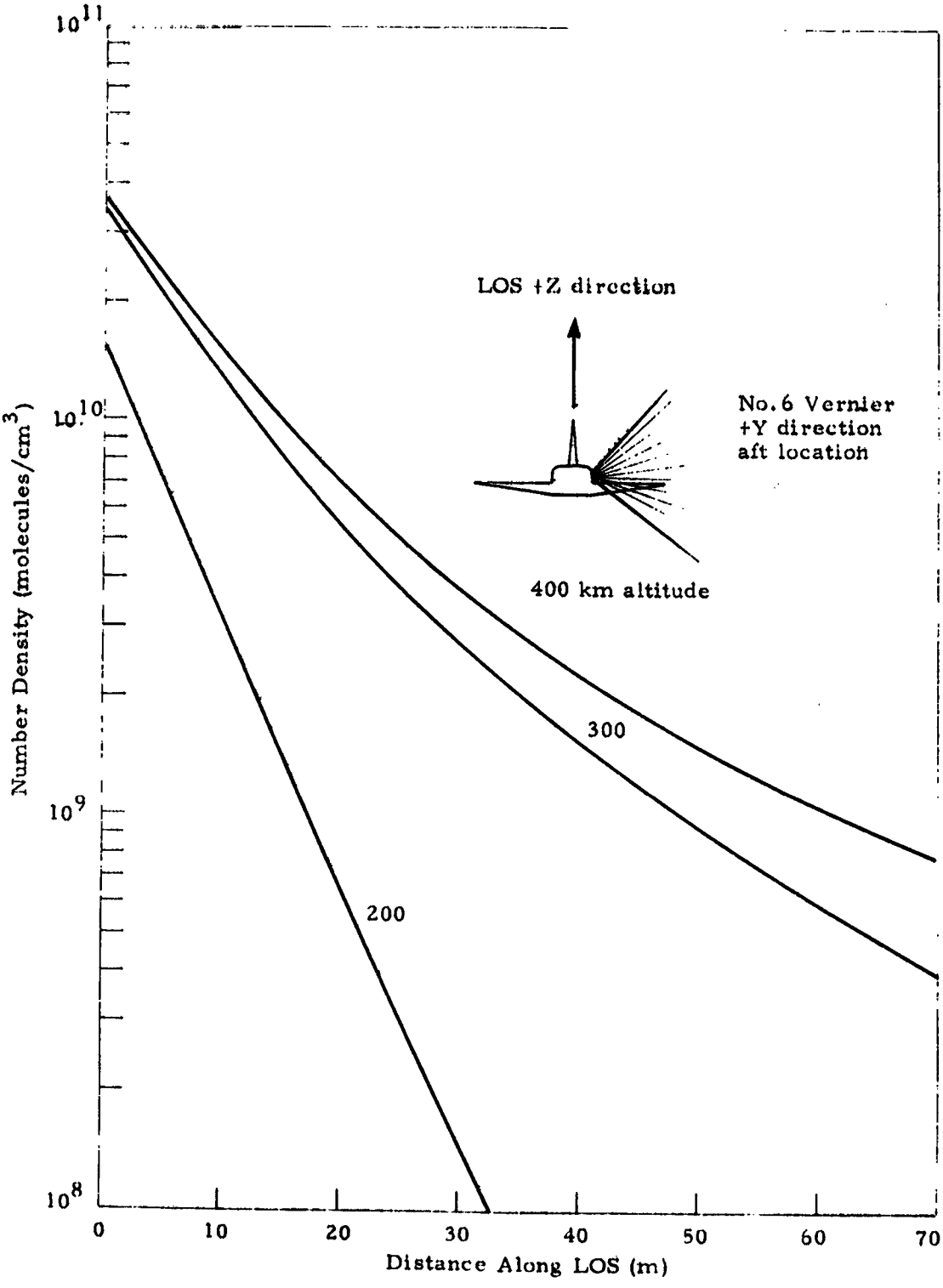

Fig. 2-5 - Computed Number Densities Along a Line-of-Sight for Various Orbit Altitudes

field and ambient atmosphere. The ambient atmosphere is seen to become a significant factor at altitudes below 300 km. The effects of shading are shown in Fig. 2-5a. It is seen that the number densities are reduced to approximately half of their original values in the region within 20 m of the PMP. The number densities are not affected much by the shading in the region farther away from the PMP.

Additional results are shown in Fig. 2-6 for the No. 6 vernier engine along a LOS in the YZ plane 60 deg from the +Z axis and these results include collisions with the jet plume and ambient atmosphere 30 deg from the +Y axis. In this case the density increases along the LOS out to about 15 m before diminishing. The increase is due to penetration of the LOS into the denser regions of the plume. Figure 2-6a shows the effects of shading. The scattered part is again seen to be cut down within 10 m of the PMP.

Results for the No. 4 vernier engine are shown in Figs. 2-7, 2-7a, 2-8 and 2-8a for the two LOSs. The scattered contribution was seen in Fig. 2-4 to increase along the LOS for about the first 5 m before diminishing. When the shading of the orbiter geometry is considered, as shown in Figs. 2-7a and 2-8a, the scattered amount is cut down for the first 10 m of the LOS. The number densities along the LOSs are dominated by the contribution due to direct flow for the first 10 m of the LOS. Dominance is then gradually taken over by the scattered flow off the wing.

Results for the flash evaporator are shown in Fig. 2-9 for both LOSs. Only the total density is shown in Fig. 2-9 because the jet is located below the wing such that there is no scattered contribution along the LOSs being considered. As noted in Fig. 2-9, the molecular flow to portions of the LOS near the spacecraft body are shadowed by the wing. The additional shadings of the fuselage and cargo bay doors completely eliminate the number densities on the LOS in the +Z direction. However, the shadings have no effect on the number densities on the LOS in the +60 deg direction.

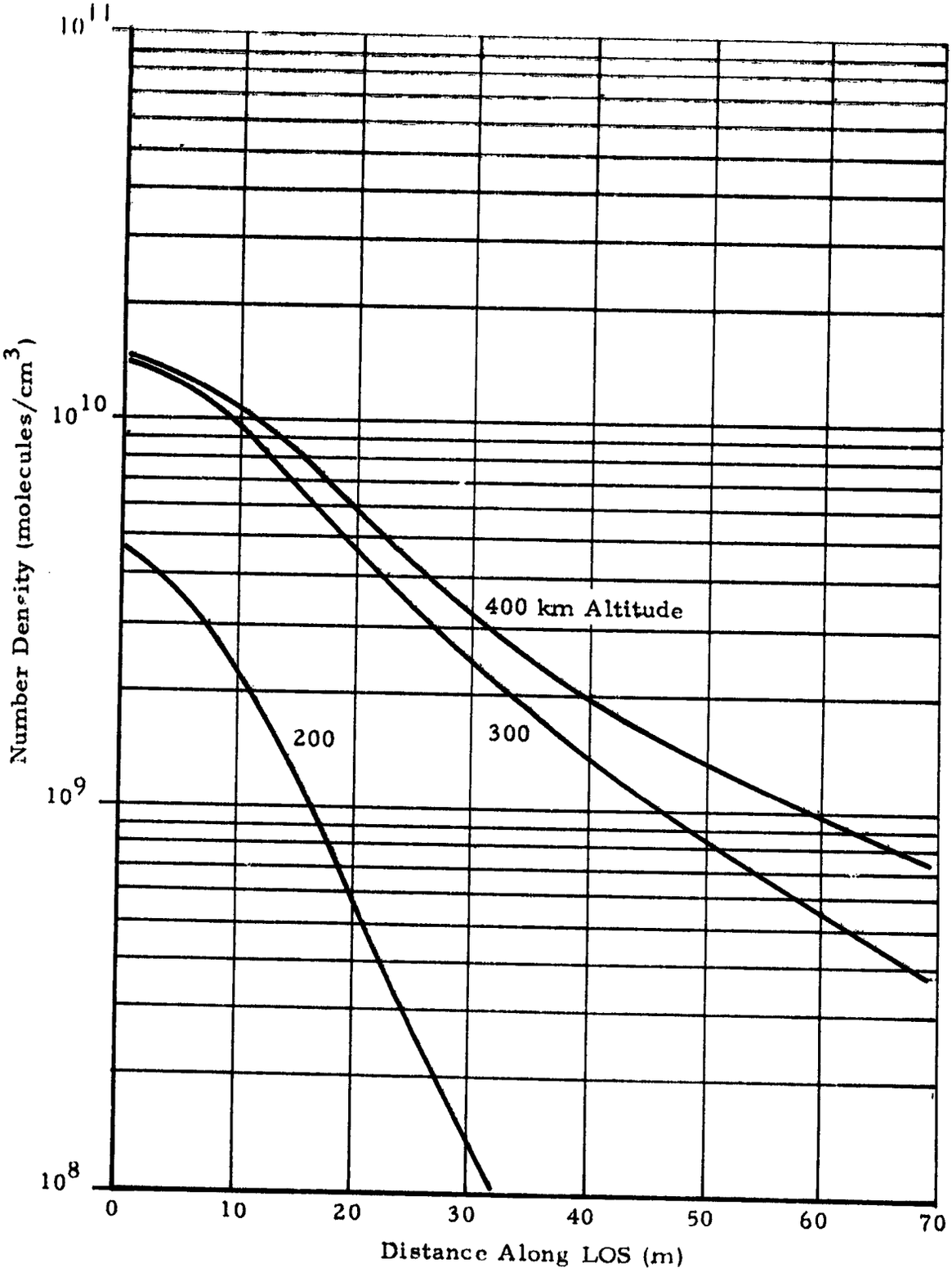

Fig. 2-5a - Computed Number Densities Along a Line of Sight for Various Orbit Altitudes with Consideration of Orbiter Geometry Shadings

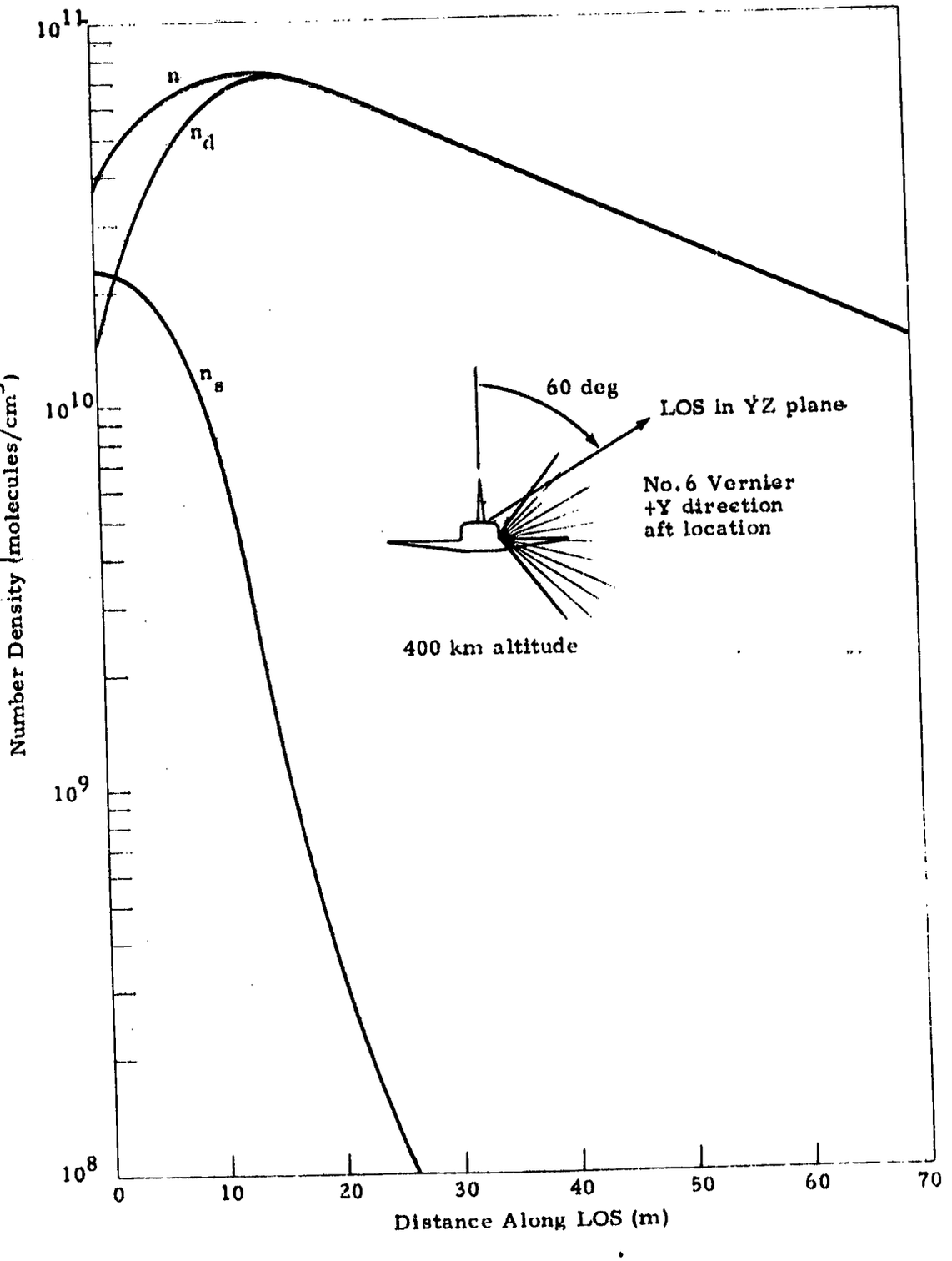

Fig. 2-6 - Computed Number Densities for the No. 6 Vernier and LOS 60 deg from +Z Axis

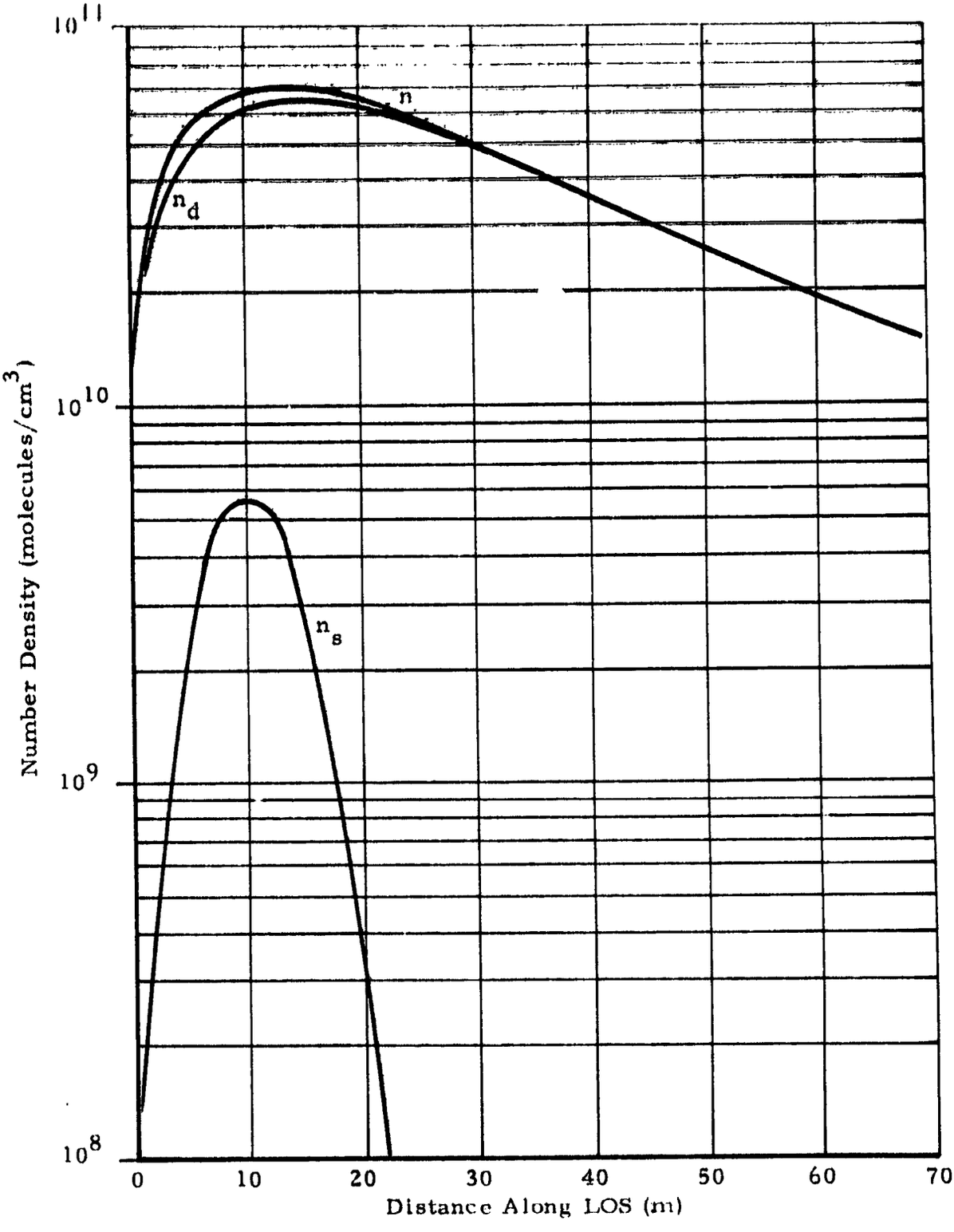

Fig. 2-6a - Computed Number Densities for the No. 6 Vernier and LOS 60 deg from +Z Axis with Orbiter Geometry Shading

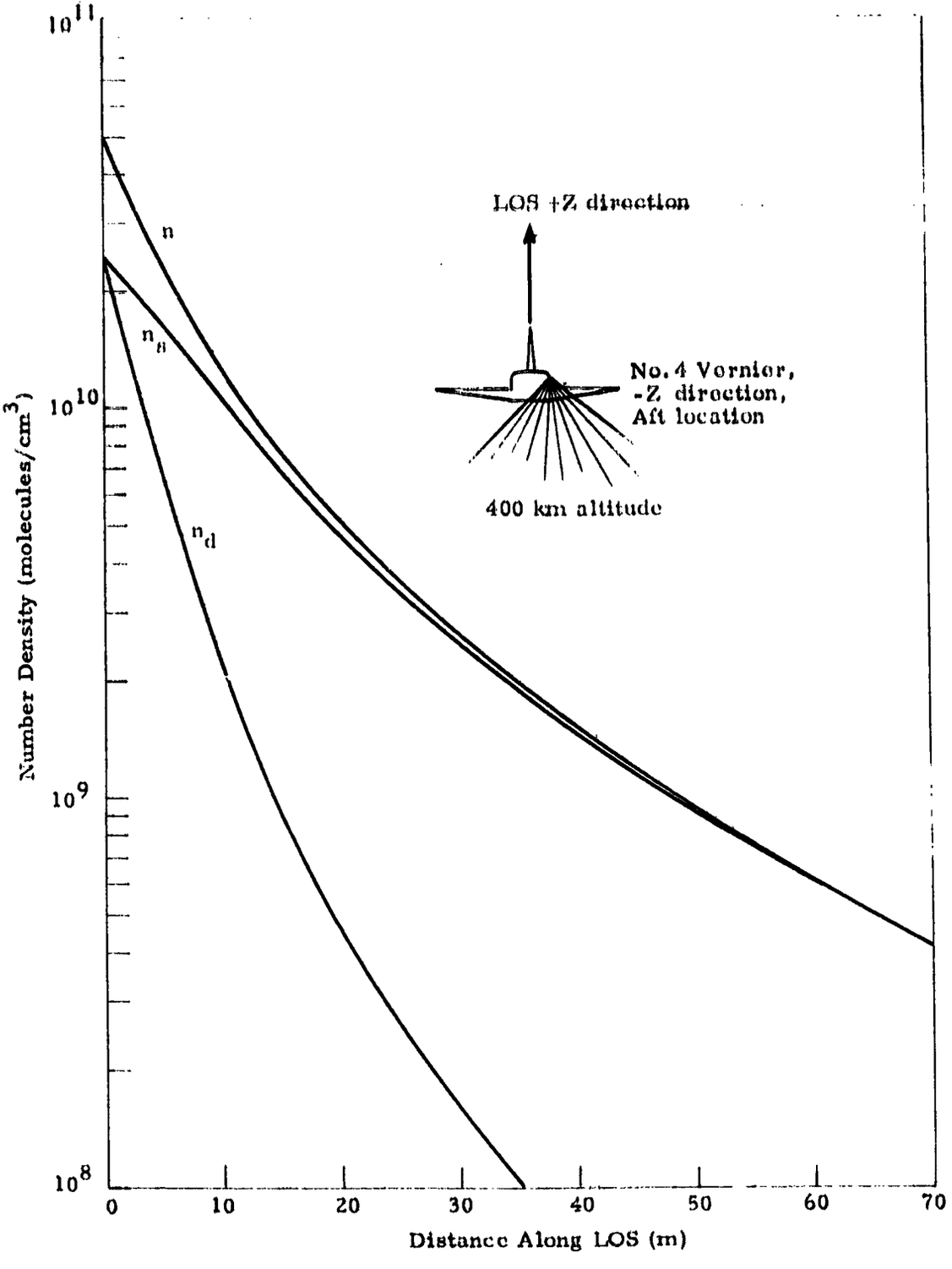

Fig. 2-7 - Computed Number Densities for the No. 4 Vernier and LOS Along the +Z Axis

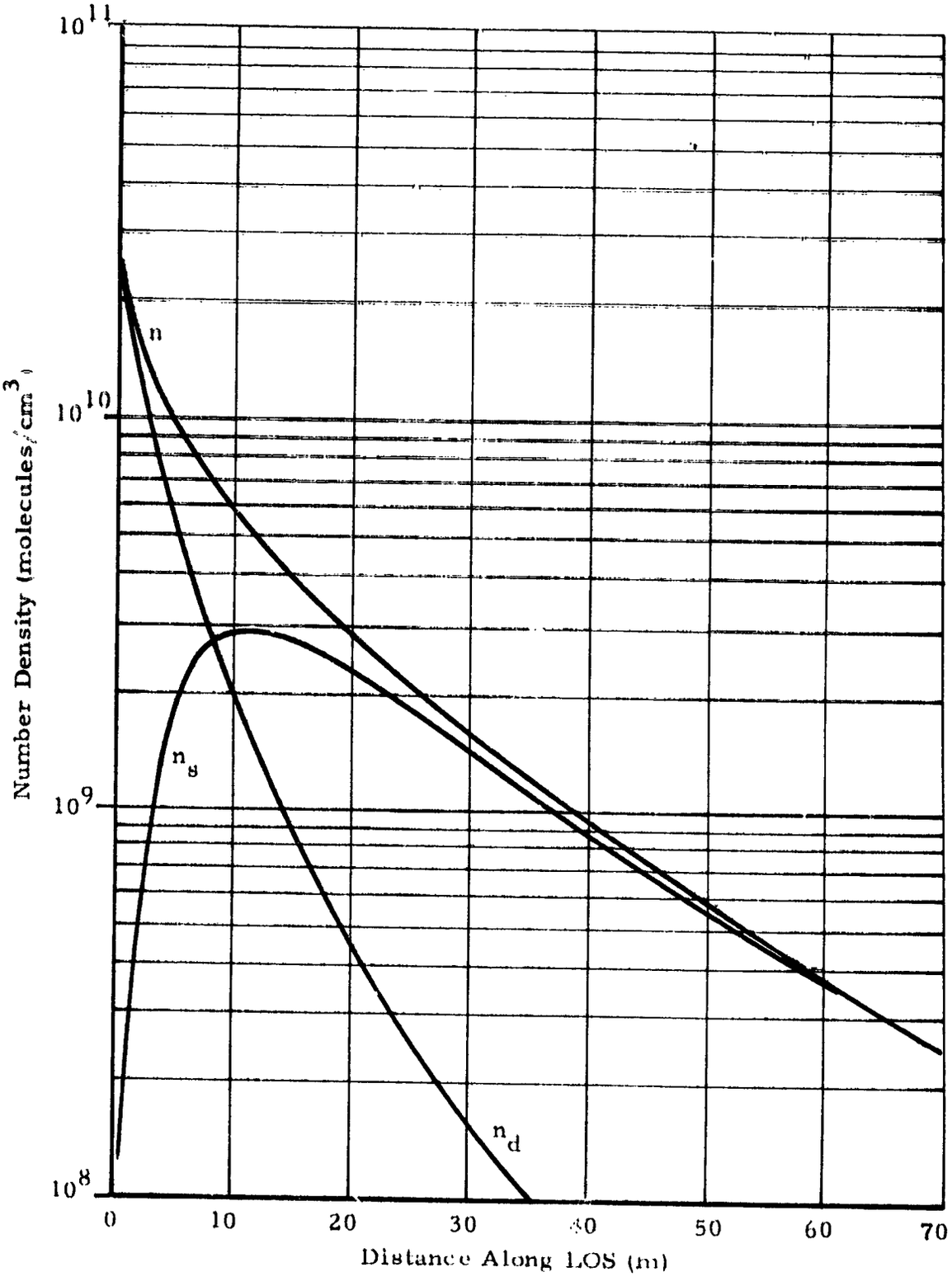

Fig. 2-7a - Computed Number Densities for the No. 4 Vernier and LOS Along the 1Z Axis with Orbiter Geometry Shading

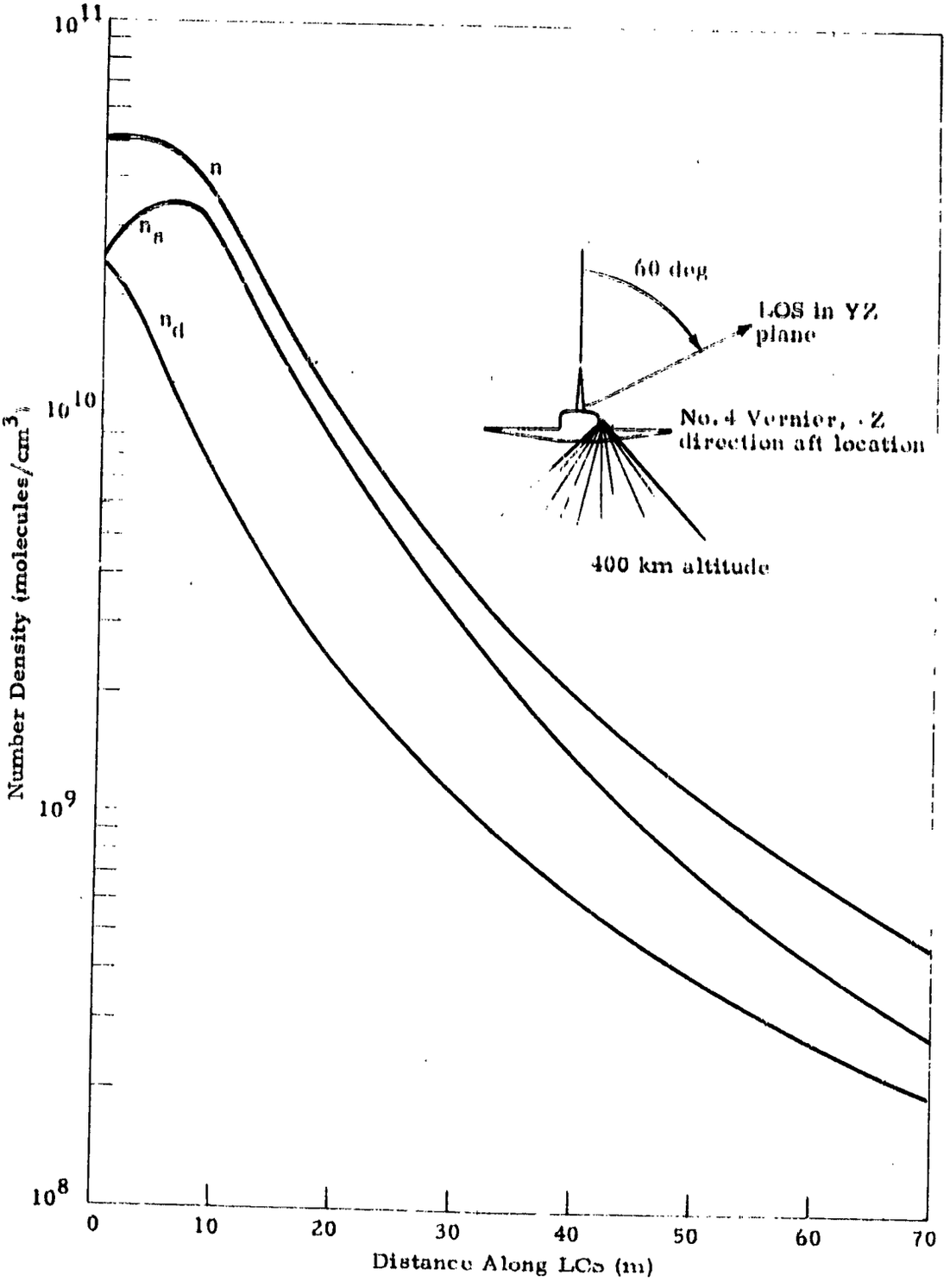

Fig. 2-8 - Computed Number Densities for the No. 4 Vernier and LOS 60 deg from +Z Axis

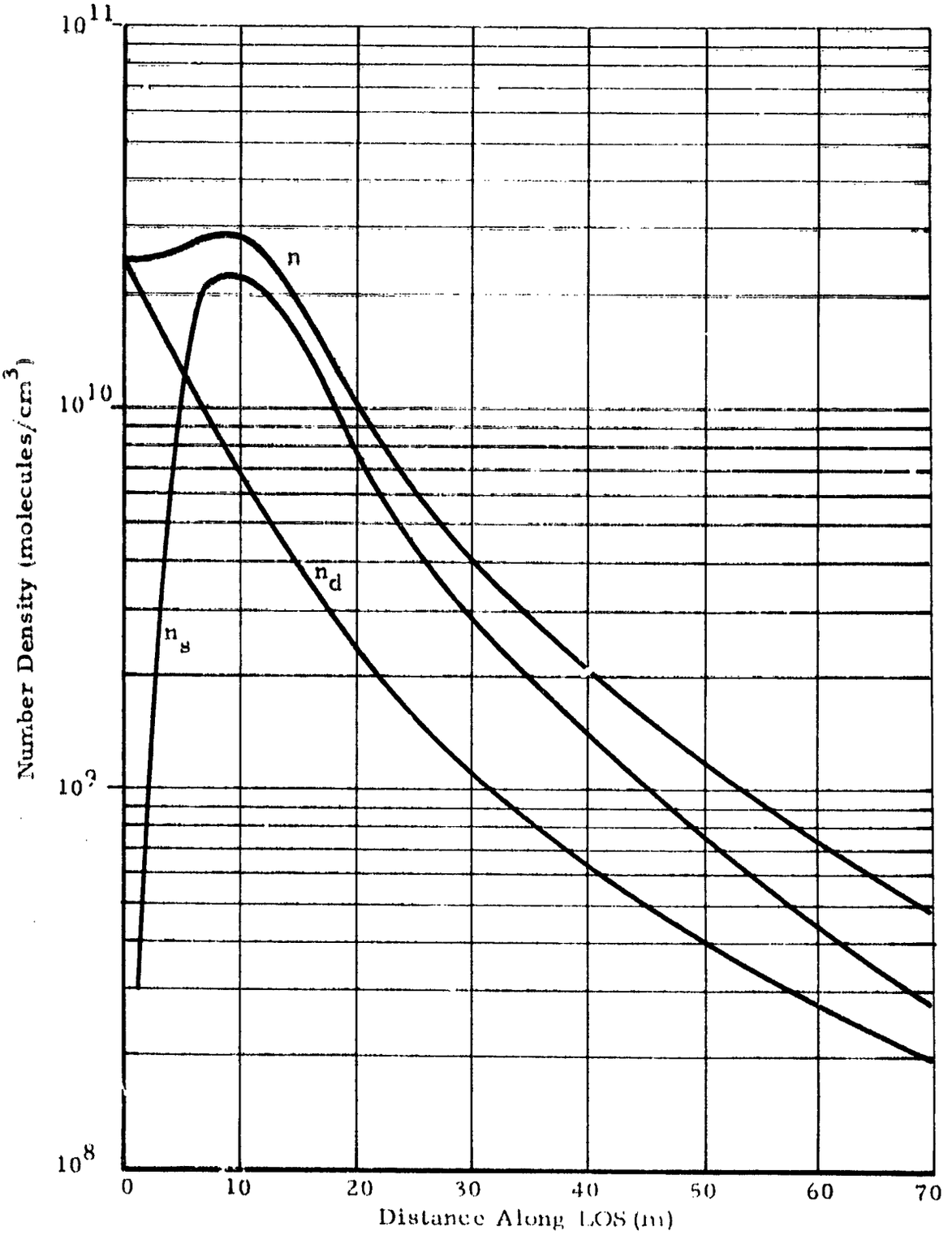

Fig. 2-8a - Computed Number Densities for the No. 4 Vernier and LOS 60 deg from +Z Axis with Orbiter Geometry Shading

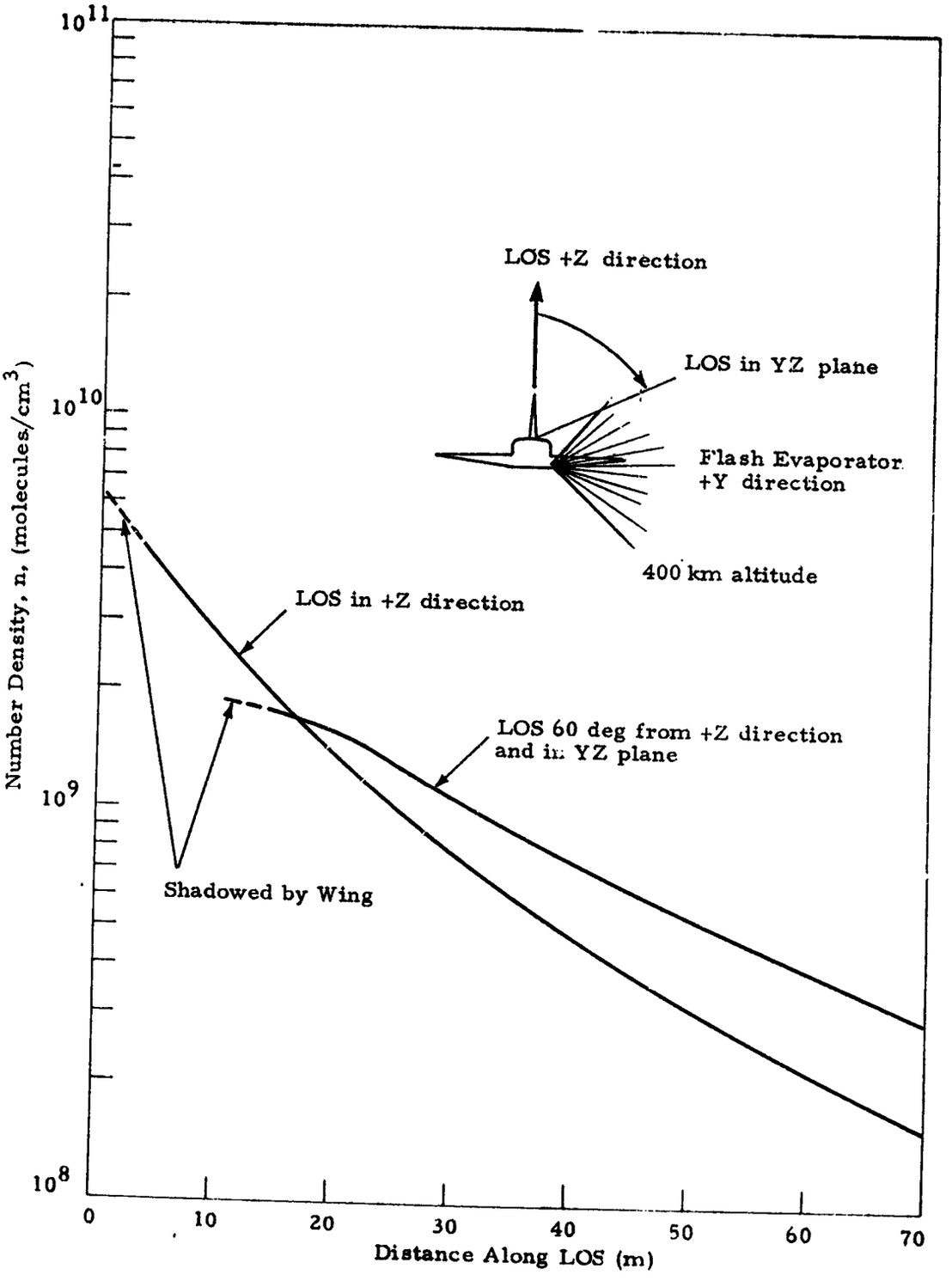

Fig. 2-9 - Computed Number Densities (Total) for the Flash Evaporator

The computed column densities are shown in Table 2-1 for all cases considered. Three values are shown for each case: (1) N includes effects of collisions with both the jet plume and ambient atmosphere, (2) N_{na} includes effects of collisions with the jet plume only, and (3) N_o includes no collision effects. The numbers in parentheses are the column densities of each case when the shading of orbiter geometry is not considered. In all cases, when the shading is not considered, the collision effects resulted in substantially lower computed column densities, as much as 90% lower for the No. 4 vernier engine and LOS in the +Z direction. A reduction of 75% is noted for the No. 6 vernier engine with LOS in the +Z direction. At this altitude (400 km), collision effects with the ambient atmosphere are seen to be relatively unimportant.

The reduction of number densities due to geometry shading effects is apparent in all vernier cases. The shadings of the cargo bay doors, fuselage and engine pods reduced substantially the contribution from the scattered flow to the vicinity within 10 m of the PMP, where the number density is highest without the shading. For the flash evaporator the number densities along the LOS are from the direct flow of the plume. The LOS in the +Z direction is completely shaded by the orbiter geometry and consequently the column density is zero. The LOS in the 60 deg direction is not affected by the additional shading.

Table 2-1

COMPUTED COLUMN DENSITIES FOR THE NOS. 4 AND 6 VERNIER ENGINES AND THE FLASH EVAPORATOR

Jet and LOS	Column Densities (molecules/cm^2) N	N_{na}	N_o
No. 6 Vernier	3.35×10^{13}	3.51×10^{13}	1.37×10^{14}
LOS +Z Direction	(5.14×10^{13})	(5.41×10^{13})	(1.99×10^{14})
No. 6 Vernier	3.12×10^{14}	3.38×10^{14}	5.23×10^{14}
LOS 60 deg from +Z Direction	(3.25×10^{14})	(3.51×10^{14})	(5.64×10^{14})
No. 4 Vernier	2.43×10^{13}	2.56×10^{13}	1.57×10^{14}
LOS +Z Direction	(4.96×10^{13})	(5.18×10^{13})	(4.17×10^{14})
No. 4 Vernier	5.95×10^{13}	6.20×10^{13}	3.82×10^{14}
LOS 60 deg from +Z Direction	(7.81×10^{13})	(8.10×10^{13})	(4.90×10^{14})
Flash Evaporator	0.0	0.0	0.0
LOS +Z Direction	(6.29×10^{12})	(7.94×10^{12})	(7.94×10^{12})
Flash Evaporator	5.11×10^{13}	6.90×10^{13}	6.90×10^{13}
LOS 60 deg from +Z Direction	(5.11×10^{13})	(6.90×10^{13})	(6.90×10^{13})

N includes molecular scattering from both plume and ambient atmosphere.

N_{na} includes molecular scattering from plume only.

N_o does not include molecular scattering.

400 km altitude. Integrated from PMP to 100 m (NR = 10).

The numbers in parentheses are the column densities without the effects of cargo bay doors, fuselage and engine pod interference.

3. BACKSCATTER FROM THE FLASH EVAPORATOR PLUME

The mass flow rate $\dot{m}$ in the flash evaporator plume flow field has been determined experimentally and is described approximately by the following empirical equation (Refs. 3 and 4).

$$\dot{m} = \frac{2.19}{r^2} (\cos\theta)^{6.272} \tag{3.1}$$

where $\dot{m}$ is in gr/cm^2/sec and r is in cm. This empirical formula is applicable only for direct flow from the nozzle in the forward direction. There will be some backscattering out of the plume in the rear direction as a result of intermolecular collisions that this formula does not account for. The study described in this section is an attempt to formulate a physically meaningful analytical technique for estimating the magnitude of this backscatter flux.

We start with the BGK kinetic model equation (Ref. 1):

$$\vec{v} \cdot \frac{\partial f}{\partial \vec{r}} = \nu (M - f) \tag{3.2}$$

where $\vec{v}$ is molecular velocity, $\vec{r}$ is the position vector, f is the velocity distribution function, ν is the local collision frequency, and M is a local equilibrium distribution function based on an elipsoidal model (Ref. 5):

$$M = n \left(\frac{m}{2\pi k T_n}\right)\left(\frac{m}{2\pi k T_s}\right)^{1/2} \exp\left[-\frac{m v_n^2}{2 k T_n} - \frac{m}{2 k T_s}(v_s - V)^2\right] \tag{3.3}$$

where n is the local number density, m is the molecular mass, k is the Boltzmann constant, V is the local mean velocity, v_s and v_n are molecular velocity components along and normal to the streamline, and T_s and T_n are temperatures corresponding respectively to the streamline and normal directions. Only two temperature components are considered because orifice flow into a vacuum is very similar to spherical source flow expansions (Ref. 6). The values of the temperature components serve as an indication of the directness of the local velocity distribution function. In spherical source flow into a vacuum, it has been shown (Ref. 6) that T_n tends toward zero as the distance from the source increases, and T_s tends toward a non-zero asymptotic value. Physically this means that there is some spread in velocities at great distances from the source, but the variations are primarily in the streamline direction.

The plume temperatures were formed by first taking moments on the BGK equation up through the second moment. This results in four differential equations in terms of the hydrodynamic quantities: density ρ, velocity V and the pressures P_s and P_n:

$$\frac{1}{\rho}\frac{d\rho}{ds} + \frac{1}{V}\frac{dV}{ds} + \frac{2}{s} = 0 \tag{3.4}$$

$$\frac{dP_s}{ds} + \rho V \frac{dV}{ds} + 2\frac{P_s - P_n}{s} = 0 \tag{3.5}$$

$$V\frac{dP_s}{ds} + 3P_s\frac{dV}{ds} + 2\frac{P_s V}{s} = \frac{P}{\eta}(P - P_s) \tag{3.6}$$

$$V\frac{dP_n}{ds} + P_n\frac{dV}{ds} + 4\frac{P_n V}{s} = \frac{P}{\eta}(P - P_n) \tag{3.7}$$

where $P = (P_s + 2P_n)/3$, η is viscosity and s is distance from the source. By manipulating these four differential equations, the following energy equation is derived:

$$\frac{3P_s + 2P_n}{\rho} + V^2 = \text{constant} \tag{3.8}$$

Defining $P_s = R\rho T_s$ and $P_n = R\rho T_n$, all of the above equations are reduced to two differential equations in terms of T_s and T_n. This pair of differential equations was numerically integrated using the Runge-Kutta technique and the results curve-fitted to yield:

For $\zeta < 1$

$$\frac{T_s}{T_o} = \frac{T_n}{T_o} = 0.283 \left(\frac{s}{D}\right)^{-\frac{4}{3}} \left[1 + 0.0943 \left(\frac{s}{D}\right)^{-\frac{4}{3}}\right] \tag{3.9}$$

For $\zeta \geq 1$

$$\frac{T_s}{T_o} = 0.000152 + \frac{0.000800}{\zeta}$$

$$\frac{T_n}{T_o} = \frac{0.0003123}{\zeta} + \frac{0.0003584}{\zeta^2} \tag{3.10}$$

where T_o is the source temperature and

$$\zeta = \frac{s}{0.03088\,(0.75)^{\kappa}\, Re^*_D} \tag{3.11}$$

where κ is the exponent in the temperature variation of viscosity (1.07 for water vapor, Ref. 7), Re^* is the throat Reynolds number of the orifice and D is the orifice diameter. The temperatures given by Eqs. (3.9) and (3.10) are used in the local distribution function given by Eq. (3.3). In deriving Eq. (3.9), the flow is assumed to be isentropic, while Eq. (3.10) is obtained assuming flow is non-isentropic far away from the orifice.

The mass flux $\dot{m}$ at a point $\vec{r}$, which is a far distance away from the flash evaporator nozzle, is found by operating on the kinetic equation:

$$\dot{m} = \int \rho \left|\vec{v}\right| \; f(\vec{v}, \vec{r}) \, d^3 \vec{v} \tag{3.12}$$

where

$$f(\vec{v}, \vec{r}) = \frac{1}{\vec{v}} \int_{\vec{r}_1'}^{\vec{r}_2'} \nu(\vec{r}') \, M(\vec{v}, \vec{r}') \exp\left[- \frac{1}{\vec{v}} \int_{\vec{r}'}^{\vec{r}_2'} \nu(\vec{r}'') \left|d\vec{r}''\right| \right] \left|d\vec{r}'\right| \tag{3.13}$$

The integration path $\vec{r}_1'$ to $\vec{r}_2'$ is across the plume in the direction out to $\vec{r}$. The end points are chosen arbitrarily to cover the significantly dense portion of the plume.

The integrations in Eqs. (3.12) and (3.13) combine to yield a volumetric integral over the significantly dense portion of the plume flow field:

$$\dot{m} = \frac{1}{r^2} \int_V \rho(\vec{r}') \, \nu(\vec{r}') \int_0^\infty v^2 \, M(\vec{v}, \vec{r}') \exp\left[- \frac{1}{v} \int_{\vec{r}'}^{\vec{r}_2'} \nu(\vec{r}'') \left|d\vec{r}''\right| \right] dv dV \tag{3.14}$$

The assumption here is that the distance r is large compared to the dimensions of the significantly dense region of the plume. The frequency $\nu(\vec{r}')$ is the local collision frequency for the production of scattered molecules, and the frequency $\nu(\vec{r}'')$ in the exponential is the collision frequency for the attenuation of the scattered beam. Accordingly, the former is given by:

$$\nu(\vec{r}') = \frac{k T(\vec{r}') \, n(\vec{r}')}{\eta(T)} \tag{3.15}$$

where $T = 1/3 \, (T_s + 2T_n)$ is the local static temperature, and the latter is given by:

$$\nu(\vec{r}'') = \frac{k T_o \, n(\vec{r}'')}{\eta(T_o)} \tag{3.16}$$

where T_o is the source, or stagnation, temperature. The stagnation temperature is used here because it is indicative of the energy of the flow field molecules with which the scattered beam collides.

The local density ρ in Eq. (3.14) is found by dividing the mass flux in (Eq. (3.1)) by the local mean velocity V, assuming the velocity has reached its thermodynamic limit given by:

$$V = \sqrt{\frac{2\gamma}{\gamma - 1} \frac{kT_o}{m}} \tag{3.16}$$

where γ is the ratio of specific heats ($\gamma = 4/3$ for water vapor).

With the above described considerations and after all of the integrations are carried out, Eq. (3.14) reduces to the following expression:

$$\dot{m} = \frac{\dot{M}}{r^2} F(\phi) \tag{3.17}$$

where $\dot{M}$ is the orifice flow rate and F is a dimensionless function of the angle ϕ formed with the jet axis. The velocity integration was evaluated numerically using the trapezoidal rules, and the volumetric integration was performed using finite elements (Ref. 8). It was found that the significantly dense region of the plume for our purposes is contained within 50 cm of the orifice location. This permits the representation of the nozzle as a point source at distances comparable to the Space Shuttle Orbiter dimensions. The results of the integration are given in Fig. 3-1. The only experimental data to compare this with was obtained in tests in a thermal/vacuum environmental chamber (Ref. 9). Multiplying their supersonic nozzle data at $\phi = 90^o$ by a factor of three to yield orifice data (Ref. 9, p. 16), we obtain the experimental data points shown in Fig. 3-1. The experimental data are higher but within an order of magnitude of the theoretical curve. Considering the conversion of supersonic nozzle data to orifice data, and the unknown contribution of scattering off test chamber surfaces, the comparison is surprisingly good.

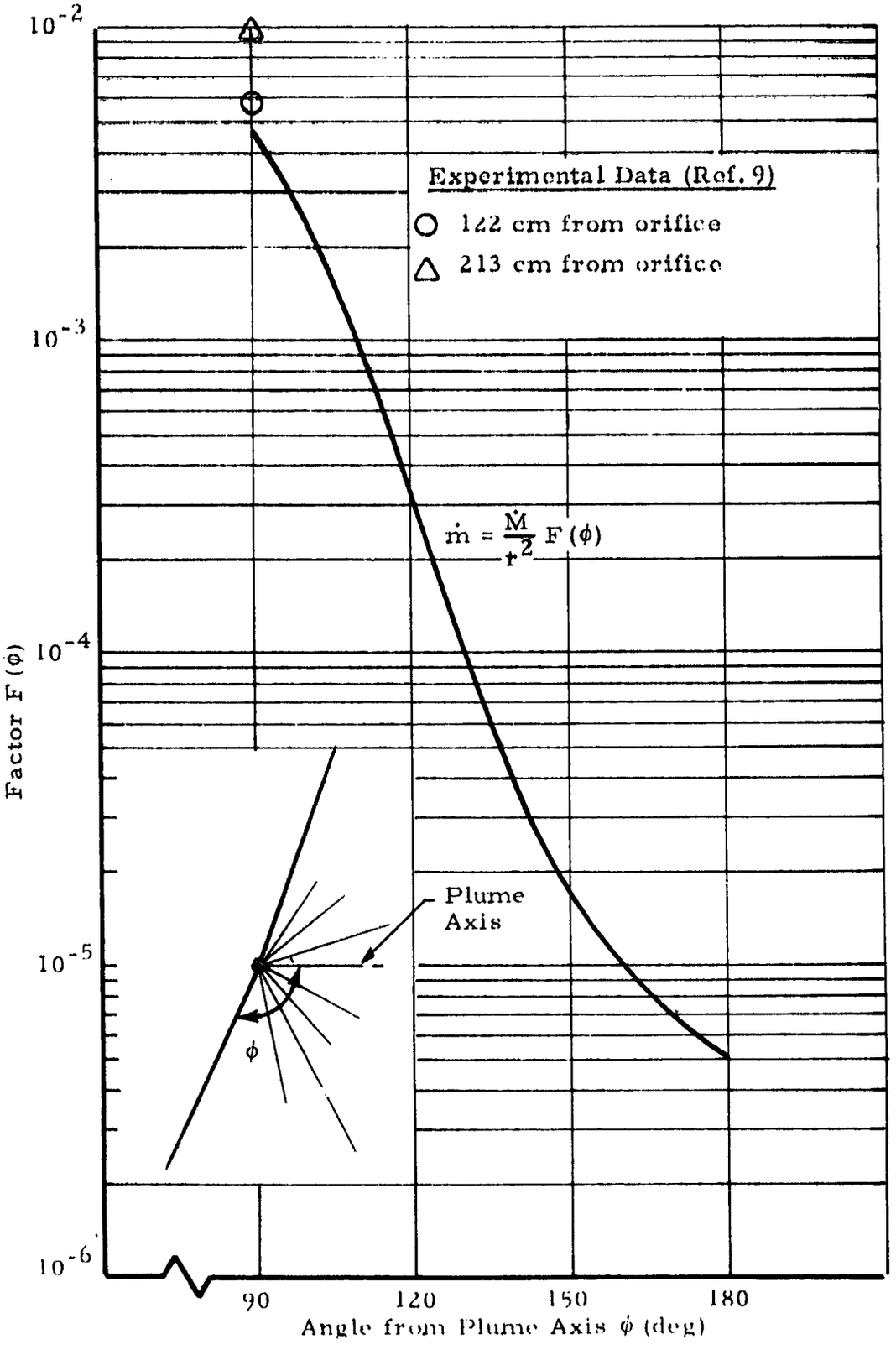

Fig. 3-1 - Predicted Far Field Backscattering for the Flash Evaporator

Based on the results obtained by the present model, an empirical formula for the far field backscattering of the flash evaporator can be constructed. This empirical formula was found to be

$$F(\phi) = 0.0002 \times 10^{1.6 \cos \frac{180(\phi - 70)}{110}} \tag{3.18}$$

with computed results shown in Fig. 3-2. Also shown in the figure are results from the empirical equation for the flash evaporator plume flow field ($\phi < 90^{\circ}$) as used in Refs. 3 and 4.

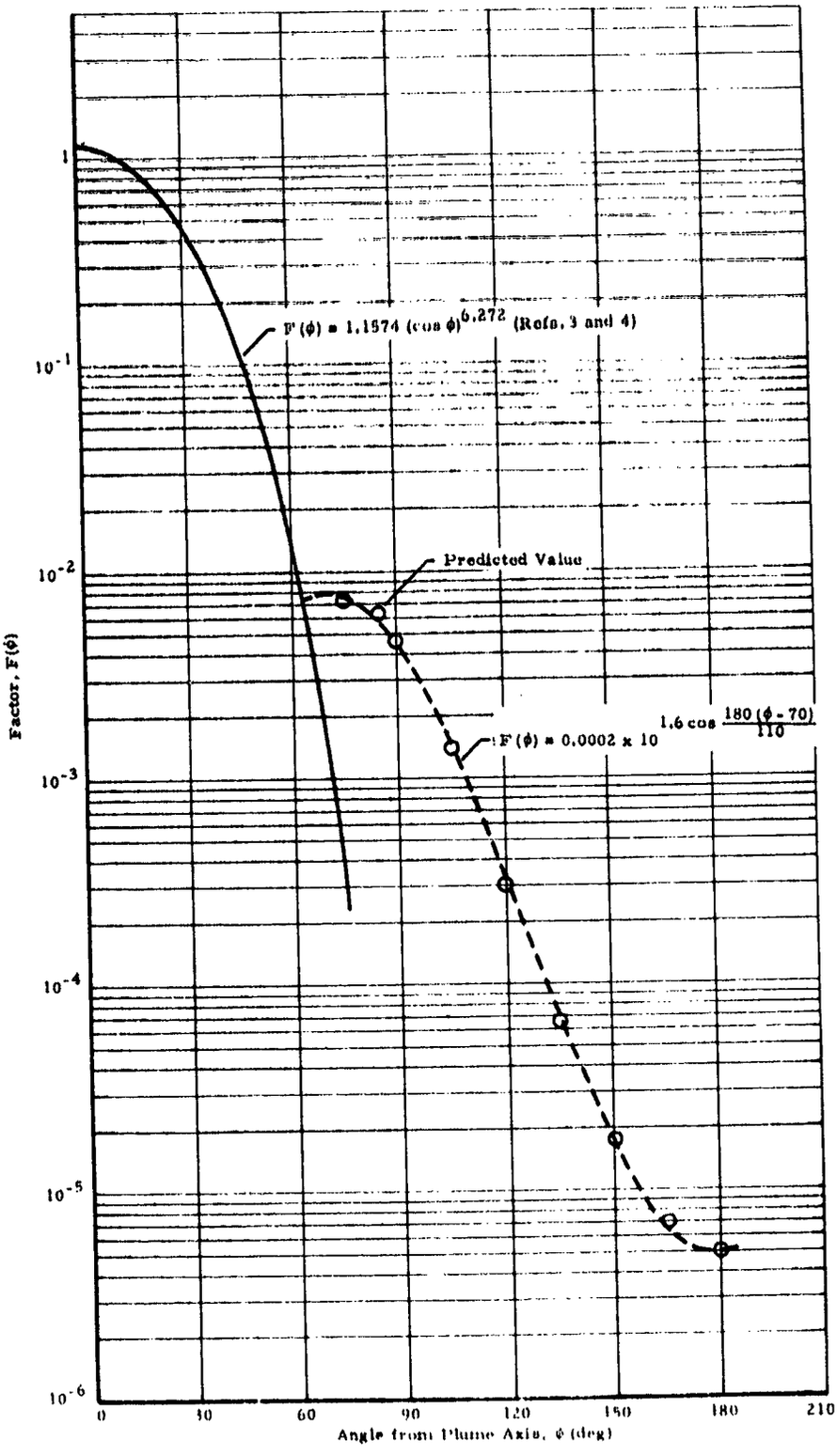

Fig. 3-2 - Empirical Formula for the Plume Flow Field and Far Field Backscattering for the Flash Evaporator

4. CONCLUSIONS

The two studies described in this report resulted in the development of practical analytical techniques for estimating the contamination environment due to molecular flow from the vernier engines and flash evaporator plumes. It was found that molecular collisions are an important factor and should be considered in calculations of scattering off the Orbiter wing surfaces. The computed column densities were shown to be reduced by as much as 90%, depending on the jet location and LOS direction, by considering attentuation of the scattered beam due to collisions with the plume flow field.

An apparently usable analytical technique was developed for estimating backscattering out of the flash evaporator plume flow field. Although the available experimental data tended to at least partially support the theoretical results, more reliable data are needed for comparison.

These studies were based on steady state conditions. The actual pulse-like character of the vernier firings and flash evaporator venting will tend to reduce the densities from the steady state values.

5. REFERENCES

1. Bhatnagar, P. L., E. P. Gross and M. Krook, "A Model for Collision Processes in Gases – I. Small Amplitude Processes in Charged and Neutral One-Component Systems," Phys. Rev. Vol. 94, No. 3, May 1954, p. 511.
2. Robertson, S. J., "Spacecraft Self-Contamination Due to Back-Scattering of Outgas Products," LMSC-HREC TR D496676, Lockheed Missiles & Space Company, Inc., Huntsville, Ala., January 1976.
3. Bareiss, L. E., R. O. Rantanen and E. B. Ress, "Payload/Orbiter Contamination Control Requirement Study," MCR-74-93, Martin Marietta Aerospace, Denver, Colo., 24 May 1974.
4. Bareiss, L. E. and E. B. Ress, "Payload/Orbiter Contamination Control Requirement Study," MCR-75-202, Martin Marietta Aerospace, Denver, Colo., 30 June 1975.
5. Holway, L. H., "Kinetic Theory of Shock Structure Using an Ellipsoidal Distribution Function," in Rarefied Gas Dynamics (J. H. de Leeuw, ed.), Academic Press, New York, 1966.
6. Hamel, B. B. and D. R. Willis, "Kinetic Theory of Source Flow Expansion with Application to the Free Jet," Phys. Fluids, Vol. 9, No. 5, May 1966, p. 829.
7. Kennard, E. H., Kinetic Theory of Gases, McGraw-Hill, New York, 1938.
8. Zienkiewicz, O. C., The Finite Element Method in Engineering Science, McGraw-Hill, New York, 1971.
9. Visentine, J. T., H.K.F. Ehlers, and B. B. Roberts, "Determination of High Velocity Water Vapor Plume Profile in a Thermal-Vacuum Environment," 7th AIAA/NASA/ASTM/IES Space Simulation Conference, Paper No. 60, Los Angeles, Calif., November 1973.